Catheter Artifact Reduction (CAR) in Dynamic Cardiac Chamber Imaging with Interventional C-arm CT

Kerstin Müller, Günter Lauritsch, Chris Schwemmer, Andreas K. Maier, Oliver Taubmann, Bernd Abt, Henning Köhler, Alois Nöttling, Joachim Hornegger and Rebecca Fahrig

***Abstract*—A C-arm CT system offers the possibility to acquire 2-D high-resolution X-ray images of the patient from different views. These projections can be used for 3-D imaging. Anatomical three-dimensional imaging holds great potential to improve cardiac interventions. However, the image acquisition using a C-arm CT system takes several seconds. A standard FDK reconstruction using all acquired projection images results in a motion blurred image. In order to improve the temporal resolution, an electrocardiogram (ECG) is acquired synchronously with the acquisition and reconstruction is performed only with subsets of projection images, each belonging to a certain heart phase. This retrospective ECG-gating of data from a single C-arm rotation provides only a few projections per heart phase for image reconstruction. This view sparsity leads to prominent streak artifacts and a poor signal-to-noise ratio. Therefore, motion estimation and correction are required for the reconstruction of the cardiac chambers. We recently presented a deformable image registration approach which allows for motion estimation on the initial ECG-gated volumes using a specifically designed imaging protocol. In this paper, an additional step to improve the initial image quality is presented which removes dense objects, i.e. pacing electrodes or catheters, before the deformable 3-D/3-D registration step. The algorithm is evaluated quantitatively and qualitatively on a simulated phantom dataset. The relative root mean square error (rRMSE) was reduced by 27 % and the universal image quality index (UQI) improved by 13 % compared to the algorithm without removing the dense objects from the reconstructions. Finally, the presented algorithmic framework was applied to a first clinical patient dataset and the preliminary results are presented in this paper.**

I. Introduction

In recent years, three-dimensional imaging has become more and more important in the field of cardiac imaging. However, most systems can only be used pre- or post-interventionally. Therefore, need for 3-D imaging directly in the catheter lab has become of major interest in the last years. Interventional 3-D imaging can be performed with an angiographic C-arm CT system already available in most catheter labs in order to perform 2-D fluoroscopic imaging. The 3-D C-arm CT image provides valuable information to the cardiologist directly inside the catheter lab, e.g. for minimally invasive valve procedures or device implantations [1]. For example, in [2], the 3-D reconstruction of the aortic root is used for guidance of a transcatheter aortic valve implantation (TAVI) by overlaying the 3-D reconstruction onto the fluoroscopic images during the deployment of the prosthesis, and for measuring critical anatomical parameters in 3-D image space.

Up to now, pre-operative three-dimensional echocardiographic volumes are used for wall motion analysis for cardiac resynchronization therapy (CRT) procedures in order to find the optimal lead position [3]. Three-dimensional C-arm reconstructions of the cardiac chambers in various heart states directly in the catheter lab would provide valuable information for the cardiologist during the CRT procedure.

For the reconstruction of a temporal sequence of 3-D cardiac images using a C-arm system, a specifically designed contrast and acquisition protocol for dynamic cardiac imaging is required [4]. Due to the design of the imaging protocol, multiple retrospectively ECG-gated reconstructions can be performed. The resulting volumes suffer from noise and streaking artifacts due to sparse view sampling. One possible solution to improve image quality is the use of all acquired projection data in combination with compensation for the cardiac motion in the reconstruction step. The cardiac motion can be estimated by registration of initial 3-D volumes of each heart phase to one reference heart phase. However, the quality of the initial images influences the accuracy of the estimated cardiac motion.

We already investigated different techniques to generate initial images for cardiac motion-estimation via deformable 3-D/3-D image registration [5]. In this paper, an additional catheter artifact removal (CAR) approach is presented to further improve the initial image quality before estimation of the cardiac motion. In our case, a contrast filled catheter and a pacing electrode are always present in the scanning field of view. The presented algorithm is applied to a simulated phantom dataset and to a first clinical patient dataset.

II. Dynamic Cardiac Imaging

In this section, the new initial image reconstruction method is described as well as the 3-D/3-D registration for cardiac motion estimation. With the estimated motion, a motion-compensated reconstruction is performed using all acquired projection images.

K. Müller, C. Schwemmer, A. K. Maier, O. Taubmann, and J. Hornegger are with the Pattern Recognition Lab, Department of Computer Science and the Erlangen Graduate School in Advanced Optical Technologies (SAOT), Friedrich-Alexander-Universität Erlangen-Nürnberg, Erlangen, Germany. Email:kerstin.mueller@cs.fau.de. G. Lauritsch, C. Schwemmer and A. Nöttling are with the Siemens AG, Healthcare Sector, Forchheim, Germany. B. Abt and H. Köhler are with the Herz- und Kreislaufzentrum, Rotenburg an der Fulda, Germany. R. Fahrig is with the Department of Radiology, Stanford University, Stanford, CA, USA.

A. 3-D Initial Image Generation

The cardiac motion is estimated on initial 3-D volumes. The initial images are reconstructed by retrospective ECG-gating. A weighting function based on the relative heart phase is introduced into the standard FDK approach, which assigns to each image an impact weight on the reconstruction result. Here, a rectangular window is used. A total of K heart phase volumes can be reconstructed. The resulting reconstructions are denoted as FDK.

Catheter Artifact Removal (CAR): Strong undersampling artifacts are caused by high-density objects like the pigtail catheter or a pacing electrode. Therefore, these objects need to be removed from the 2-D projection images before the reconstruction. The high density objects are identified in the ECG-gated volumes to generate binary 3-D mask volumes for each heart phase. The segmentation process is restricted to a user-defined region of interest (ROI). A thresholding operation is applied with a threshold determined as the mean value inside the defined ROI. The segmented pixels are dilated by a circular object with a radius of 1 voxel. The resulting mask volumes are forward projected into the 2-D projection images which belong to the corresponding heart phase. The 2-D mask images combined with the log-transformed projection images are used for catheter removal. In this paper, a low-frequency-based object masking called Subtract-and-Shift (SaS) is used for the removal of the catheter in the 2-D projection images [6]. The algorithm makes use of the fact that many dense objects do not absorb all incident radiation. Therefore, some remaining anatomical structure is still available within the region overlaid by the object and should be used by an interpolation algorithm.

The resulting projection images are used for ECG-gated filtered backprojection reconstruction to provide volumes without catheters and electrodes. These reconstructions using the catheter removed projections are denoted as cathFDK.

B. Cardiac Motion Estimation

In order to estimate the cardiac motion, one heart phase needs to be chosen as reference phase. The corresponding volume is the reference volume and all other volumes are registered separately to the reference volume. The 3-D motion vector field is derived by optimizing an objective function $\mathcal{L}_{NCC}(\widetilde{\boldsymbol{s}}_{\text{mm}})$, with the vector $\widetilde{\boldsymbol{s}}_{\text{mm}} \in \mathbb{R}^{\widetilde{K}_{\text{mm}}}$ denoting the motion model parameters between two heart phases, such that the negative normalized cross correlation (NCC) between the (catheter removed) ECG-gated volumes is minimized. The optimization is performed with an adaptive stochastic gradient descent optimizer. The motion is parameterized by cubic third-order B-splines with uniformly spaced control points $C_s \times C_s \times C_s$. Every control point has its own parameter vector, defining the number of motion model parameters as $\widetilde{K}_{\text{mm}} = 3(C_s + 3)^3$. In order to estimate the cardiac motion over the whole scan, the optimization needs to be performed between all $K-1$ heart phases, resulting in an overall motion vector dimension $K_{\text{mm}} = (K-1)\,\widetilde{K}_{\text{mm}}$. In this paper, a toolbox for nonrigid registration of medical images called `elastix` is used for the 3-D/3-D motion estimation [7]. A multi-resolution scheme of 4 levels is used with a sampling factor of 2 on each pyramid level. At the highest image resolution a number of $C_s = 16$ control points are used in each spatial dimension.

C. Motion-compensated Reconstruction

The estimated motion vector field is incorporated into a voxel-driven filtered backprojection reconstruction algorithm which compensates for the motion [8]. The motion correction is applied during the backprojection step by shifting the voxel to be reconstructed according to the motion vector field.

Using no catheter removal for the initial volume reconstruction, the resulting motion-compensated reconstructed volumes are denoted as FDK-MC. When the CAR approach is used for the initial image reconstruction and motion estimation, but the motion-compensated reconstruction is performed with the original measured projection images, the reconstruction is denoted as cathFDK-MC. If the motion-compensated reconstruction utilizes the projection images without catheters and electrodes, the volumes are denoted as cathFDK-MC$_i$.

III. Experiments

A. Phantom Model

A ventricle dataset [9], [10] of a similar design to the XCAT phantom [11] was created. The phantom dataset was simulated with a polychromatic X-ray spectrum. We used a source spectrum $E(b)$ with 36 energy bins from 10 keV to 90 keV, and a time-current product of 2.5 mAs per X-ray pulse. A catheter was simulated coming from the aorta into the left ventricle. The same deformation as for the heart was applied to the catheter. The material of the catheter is similar to copper in order to induce severe streak artifacts in the reconstructions. The material properties of the catheter, bones and the bone marrow have the were chosen according to the mass attenuation coefficients of the NIST X-Ray Table[1]. All other structures are assumed to have the same absorption behavior as water with different densities similar to the FORBILD phantom[2]. The density of the contrasted left ventricle bloodpool was set to 2.5 g/cm^3, the density of the myocardial wall to 1.5 g/cm^3 and the contrasted blood in the aorta to 2.0 g/cm^3. Poisson distributed noise was added to the simulated projection stacks such that the noise characteristics of the reconstructed images fit those of the clinical data. As gold standard, static projection images of the phantom with a catheter were generated without noise. The phantom projection data and geometry are publicly available and can be downloaded from *https://conrad.stanford.edu/data/heart*.

The phantom dataset was simulated with similar parameters as used for clinical acquisitions of porcine models [5], [4]. The acquisition simulation was performed over 14.5 s capturing 381 projection images at an angular increment of 0.52° during one C-arm sweep. The isotropic pixel resolution was 0.31 mm/pixel (0.19 mm in isocenter) and the detector size 1240 × 960 pixels. The heart rate was set to 131 bpm. For the phantom dataset, a strict gating was performed, i.e. only one projection per heart cycle is used for reconstruction. A total of 32 heart cycles were acquired resulting in 12 reconstructed

[1] http://physics.nist.gov/PhysRefData/Xcom/html/xcom1.html
[2] http://www.imp.uni-erlangen.de/phantoms/thorax/thorax.htm

Table I: The rRMSE and UQI of the dynamic phantom model with a catheter for all $K = 12$ heart phases as mean and standard deviation.

Method	rRMSE	UQI
FDK-MC	0.85 ± 0.34	0.84 ± 0.01
cathFDK-MC	0.62 ± 0.43	0.94 ± 0.01
cathFDK-MC$_i$	0.58 ± 0.52	0.97 ± 0.01

heart phases. Image reconstruction was performed on an image volume of (25.6 cm)^3 distributed on a 256^3 voxel grid.

B. Clinical Data

A clinical patient dataset acquisition was performed using an Artis zeego system (Siemens AG, Healthcare Sector, Forchheim, Germany). The acquisition time was 14 s capturing 381 projection images with 26 f/s at an angular increment of 0.52° during one C-arm rotation. The isotropic pixel resolution was 0.31 mm/pixel (0.19 mm in isocenter) and the detector size 1240 × 960 pixels. The heart rate was stimulated through external heart pacing to 115 bpm, which is lower than the frequency used for the phantom model (131 bpm). The width of the gating window was set to 10 % of the heart cycle, resulting in ≈ 34 projections for the reconstruction of an initial image at a specific heart phase. For this dataset, 10 heart phase volumes were reconstructed at a phase increment of 10 %. A volume of 91 ml undiluted contrast agent fluid was administered in the pulmonary artery at a speed of 7 ml/s beginning 13 s before the X-ray rotation was started. The X-ray delay was determined by a test bolus injection. Image reconstruction was performed on an image volume of (25.6 cm)^3 distributed on a 256^3 voxel grid.

IV. Results and Discussion

A. Phantom Model

For the dynamic phantom data, the 3-D error and a quantitative 3-D image metric can be evaluated. The gold standard image of the non-gated FDK reconstruction using all projections of the static heart phantom of the same heart phase is shown in Fig. 1a. The error as well as the image quality metric were evaluated inside a volume of interest around the ventricle. The region of the catheter was also excluded from the evaluation, since the catheter motion was not in the focus of the cardiac chamber imaging. The relative root mean square error (rRMSE) was used to quantify the 3-D reconstruction error. The results were averaged over all heart phases, resulting in an overall rRMSE. As a 3-D image quality metric the universal image quality index (UQI) was computed [12]. The UQI ranges from -1 to 1, with 1 as the best overlap between both reconstructions. All results were averaged over the heart phases, resulting in the overall UQI. Looking at the quantitative results in Table I, the cathFDK-MC$_i$ and the cathFDK-MC outperform the FDK-MC reconstructions. For the cathFDK-MC$_i$, the rRMSE is reduced by 27 % and the universal image quality index (UQI) improved by 13 % compared to FDK-MC.

The reconstruction results for the phantom data are shown in Fig. 1 for a heart phase of 30 %. The non-gated FDK reconstruction suffers from motion blurring artifacts as can be seen in Fig. 1b. The catheter causes severe streak artifacts in the ECG-gated reconstructions (Fig. 1c). Motion compensation does not eliminate these streak artifacts since the motion estimation is disturbed by them (Fig. 1d). The cathFDK (Fig. 1e) shows less streak artifacts and consequently the corresponding motion compensated image shows a much better image quality (Fig. 1f). In Fig. 1g, the cathFDK-MC$_i$ result is presented, only minor streaking artifacts are visible in the reconstruction. As a post-processing step, the segmented catheter can be added to the cathFDK-MC$_i$ reconstruction (Fig. 1h).

B. Clinical Data

The reconstruction results for the clinical patient dataset are presented in Fig. 2 for a systolic and a diastolic heart phase. It can be seen that artifacts overlay small left ventricular structures in the systolic and diastolic ECG-gated FDK reconstructions (cf. Fig. 2a and 2b, indicated by the arrows). The image quality of the motion-compensated reconstructions using cathFDK-MC$_i$ is improved considerably compared to the initial images (cf. Fig. 2c and 2d).

V. Summary and Conclusion

For cardiac image acquisition with a C-arm CT, it is necessary to include the cardiac motion in the reconstruction. In this paper, we have presented cardiac motion estimation from initial 3-D volume data sets with a deformable B-spline registration. If a dense object is present inside the scan field of view, the undersampled ECG-gated initial images suffer from streak artifacts which disturb the motion estimation. The shadow of the dense object has to be removed from the 2-D projection images as a preprocessing step before the reconstruction of the initial images. Using these volumes, motion is estimated with an improved accuracy. No further image enhancement and processing is needed. For motion-compensated reconstruction of sparse structures like the catheter, different algorithms can be used [13]. The phantom simulation study shows quantitatively the benefit of the proposed method. Clinical preliminary motion-compensated reconstructions of a patient dataset are promising.

Disclaimer: The concepts and information presented in this paper are based on research and are not commercially available.

Acknowledgment

The authors gratefully acknowledge funding support from the NIH grant R01 HL087917 and of the Erlangen Graduate School in Advanced Optical Technologies (SAOT) by the German Research Foundation (DFG) in the framework of the German excellence initiative.

References

[1] H. Hetterich, T. Redel, G. Lauritsch, C. Rohkohl, and J. Rieber, "New x-ray imaging modalities and their integration with intravascular imaging and interventions," *Int J Cardiovasc Imaging*, vol. 26, no. 7, pp. 797–808, October 2010.

[2] M. John, R. Liao, Y. Zheng, A. Nöttling, J. Boese, U. Kirschstein, J. Kempfert, and T. Walther, "System to guide transcatheter aortic valve implantations based on interventional C-arm CT imaging," in *MICCAI 2010*, vol. 6361, September 2010, pp. 375–382.

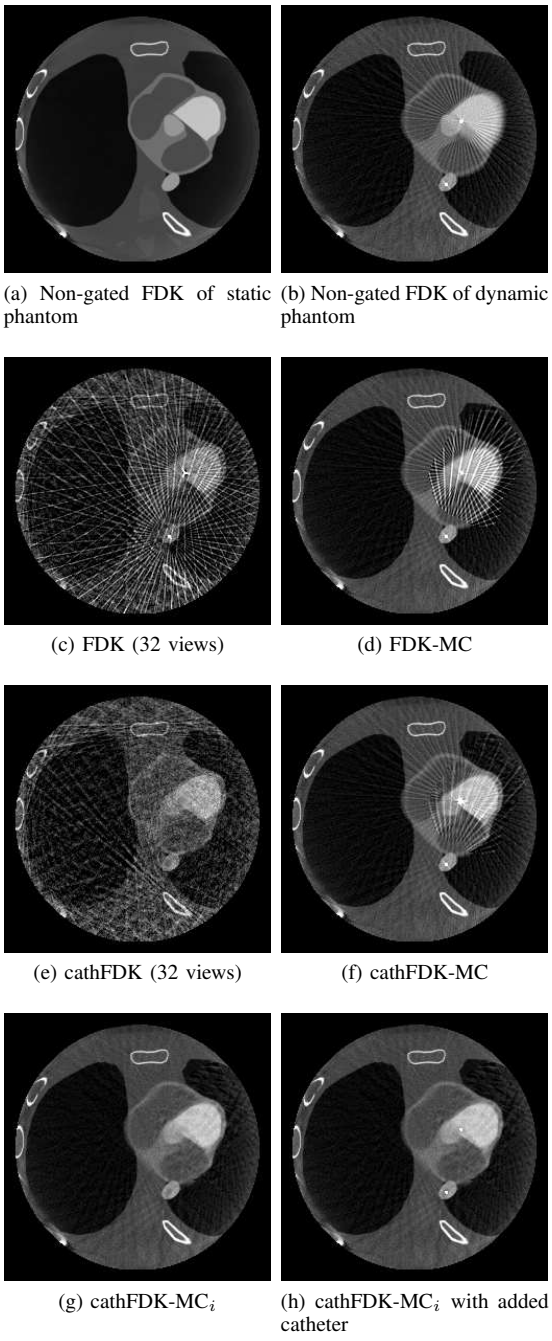

(a) Non-gated FDK of static phantom

(b) Non-gated FDK of dynamic phantom

(c) FDK (32 views)

(d) FDK-MC

(e) cathFDK (32 views)

(f) cathFDK-MC

(g) cathFDK-MC$_i$

(h) cathFDK-MC$_i$ with added catheter

Figure 1: Central slice of initial volumes and motion-compensated reconstructions of the phantom model with a catheter and a relative heart phase of $\approx 30\,\%$ (W 3100 HU, C 780 HU, slice thickness 1 mm).

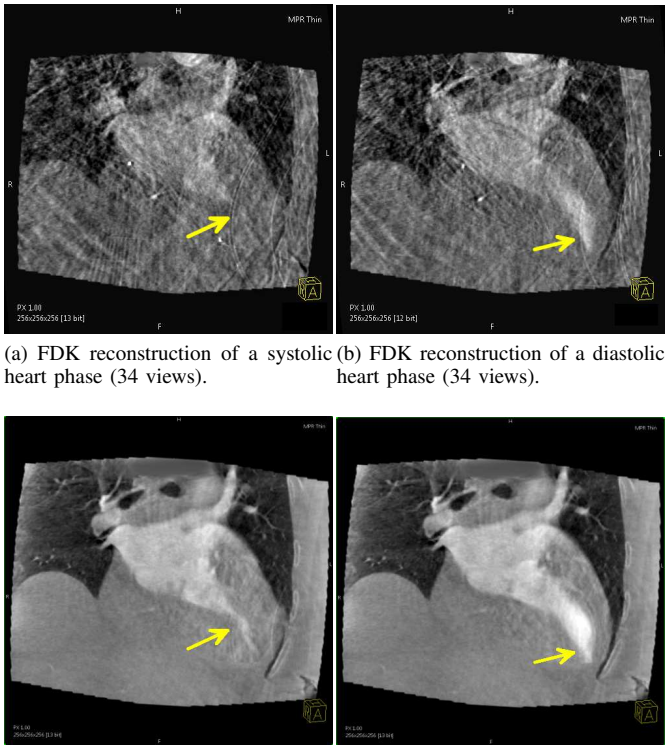

(a) FDK reconstruction of a systolic heart phase (34 views).

(b) FDK reconstruction of a diastolic heart phase (34 views).

(c) cathFDK-MC$_i$ of a systolic heart phase.

(d) cathFDK-MC$_i$ of a diastolic heart phase.

Figure 2: First results of a clinical patient dataset with the cathFDK-MC$_i$ reconstruction of a systolic and diastolic heart phase (W 2080 HU, C 113 HU, slice thickness 1 mm).

[3] M. Döring, F. Braunschweig, C. Eitel, T. Gaspar, U. Wetzel, B. Nitsche, G. Hindricks, and C. Piorkowski, "Individually tailored left ventricular lead placement: lessons from multimodality integration between three-dimensional echocardiography and coronary sinus angiogram," *Europace*, vol. 15, no. 5, pp. 718–727, May 2013.

[4] S. De Buck, D. Dauwe, J.-Y. Wielandts, P. Claus, C. Koehler, Y. Kyriakou, S. Janssens, H. Heidbuchel, and D. Nuyens, "A new approach for prospectively gated cardiac rotational angiography," in *Proceedings of SPIE Medical Imaging 2013*, vol. 8668, February 2013.

[5] K. Müller, C. Schwemmer, G. Lauritsch, C. Rohkohl, A. Maier, H. Heidbüchel, S. De Buck, D. Nuyens, Y. Kyriakou, C. Köhler, R. Fahrig, and J. Hornegger, "Image artifact influence on motion compensated tomographic reconstruction in cardiac C-arm CT," in *Proceedings of the Fully3D*, June 2013, pp. 98–101.

[6] C. Schwemmer, M. Prümmer, V. Daum, and J. Hornegger, "High-density object removal from projection images using low-frequency-based object masking," in *Bildverarbeitung für die Medizin 2010 - Algorithmen - Systeme - Anwendungen*, March 2010, pp. 365–369.

[7] S. Klein, M. Staring, K. Murphy, M. Viergever, and J. Pluim, "elastix: a toolbox for intensity based medical image registration," *IEEE Trans Med Imaging*, vol. 29, no. 1, pp. 196–205, 2010.

[8] D. Schäfer, U.fer, J. Borgert, V. Rasche, and M. Grass, "Motion-Compensated and Gated Cone Beam Filtered Back-Projection for 3-D Rotational X-Ray Angiography," *IEEE Trans Med Imaging*, vol. 25, no. 7, pp. 898–906, July 2006.

[9] A. Maier, H. Hofmann, M. Berger, P. Fischer, C. Schwemmer, H. Wu, K. Müller, J. Hornegger, J.-H. Choi, C. Riess, A. Keil, and R. Fahrig, "Conrad - a software framework for cone-beam imaging in radiology," *Med Phys*, vol. 40, no. 11, pp. 111 914–1–8, November 2013.

[10] K. Müller, A. Maier, P. Fischer, B. Bier, G. Lauritsch, C. Schwemmer, R. Fahrig, and J. Hornegger, "Left ventricular heart phantom for wall motion analysis," in *Proceedings of the IEEE NSS/MIC 2013*, October 2013.

[11] W. Segars, M. Mahesh, T. Beck, E. Frey, and B. Tsui, "Realistic CT simulation using the 4D XCAT phantom," *Med Phys*, vol. 35, no. 8, pp. 3800–3808, August 2008.

[12] Z. Wang and A. Bovik, "A universal image quality index," *IEEE Signal Proc Let*, vol. 9, no. 3, pp. 81–84, March 2002.

[13] C. Schwemmer, C. Rohkohl, G. Lauritsch, K. Müller, and J. Hornegger, "Residual Motion Compensation in ECG-Gated Interventional Cardiac Vasculature Reconstruction," *Phys Med Biol*, vol. 58, no. 11, pp. 3717–3737, June 2013.